**SUPPORTING INFORMATION**

# Olivine dissolution in seawater: implications for $CO_2$ sequestration through Enhanced Weathering in coastal environments

***Francesc Montserrat*[*,1,6], *Phil Renforth*[2], *Jens Hartmann*[3], *Martine Leermakers*[2], *Pol Knops*[4] and *Filip J.R. Meysman*[1,5]**

(*) Corresponding Author, montserrat@usp.br, f.montserrat@gmail.com ;
(1) Department of Analytical and Environmental Chemistry, Free University of Brussels, Pleinlaan 2, 1050, Brussels, Belgium;
(2) School of Earth and Ocean Sciences, Cardiff University, Main Building, Park Place, Cardiff, CF10 3AT, United Kingdom;
(3) Department of Geochemistry, University of Hamburg, Bundesstrasse 55, 20146, Hamburg, Germany;
(4) Green Minerals B.V. , Boulevard 17, 6127 AX, Grevenbicht, The Netherlands;
(5) Aarhus Institute of Advanced Studies (AIAS), Aarhus University, Hoegh-Guldbergs Gade 6B, DK-8000 Aarhus C, Denmark
(6) Current Address: Department of Marine Ecology, Management and Conservation, Institute for Oceanography – University of São Paulo, Praça do Oceanográfico 191, 05508-120, São Paulo (SP), Brazil

## Table of Contents

## SI 1: Olivine dissolution

The dissolution of olivine in an aqueous environment consumes protons or equally increases the alkalinity, as shown here for forsterite, the Mg-rich endmember of olivine:

(1) $Mg_2SiO_4 + 4H^+ \rightarrow 2Mg^{2+} + H_4SiO_4$

The resulting alkalinisation of the pore solution causes atmospheric $CO_2$ to be transferred to the water phase. Dissolved $CO_2$ forms true carbonic acid ($H_2CO_3$), which subsequently dissociates into bicarbonate and carbonate ions:

(2) $CO_2\,(g) \rightarrow CO_2\,(aq) + H_2O \rightarrow H_2CO_3 \rightarrow HCO_3^- + H^+ \rightarrow CO_3^{2-} + H^+$

The overall dissolution reaction equation can be written as:

(3) $Mg_2SiO_4 + 4H_2O + 4CO_2\,(g) \rightarrow 2Mg^{2+} + 4HCO_3^- + H_4SiO_4$

According to this idealized stoichiometry, 4 mol of atmospheric $CO_2$ are sequestered as dissolved bicarbonate for every mol of olivine dissolved. In reality, this ratio is closer to 3.0 – 3.5 due to buffering effects in the carbonate system of natural waters [1,2] (see main text for detailed discussion).

## SI 2: Composition of solid minerals and seawater media

The olivine sand originated from the Åheim quarry (Norway) and was obtained from greenSand (The Netherlands). The composition of the olivine was analyzed by ICP-OES (ThermoFischer iCAP 6000), following dissolution with Aqua Regia, providing a molar Mg:Fe ratio of 0.94:0.06 and characterizing the olivine as Forsterite-94 ($Fo_{94}$). The Ni content was estimated as 0.0075 mol Ni $mol^{-1}$ olivine. While the mass fraction of the cations (mole per mol of olivine) was calculated from the ICP-OES, the remaining mass fraction was attributed to silicate ($SiO_4$). The chemical composition is specified in Table S1.

The grain size distribution of the olivine sand was measured by laser diffraction on a Malvern Mastersizer 2000 (mean ± SD are reported with n=6; Table S2). The olivine sand had a median grainsize ($D_{50}$) of 143 ± 0.18 µm, with $D_{10}$ and $D_{90}$ quantiles of 91 ± 0.13 and 224 ± 0.29 µm, respectively, and contained less than 0.4 % of particles < 63 µm. A specific surface area $A_{BET}$ = 0.295 ± 0.13 $m^2\ g^{-1}$ (n=12) was determined via nitrogen ($N_2$) gas adsorption using the BET-method. For reference, the specific surface area of spherical particles with a particle size distribution (PSD), based on the same median grainsize ($D_{50}$ = 143 µm), was calculated as $A_{GEO}$ = 0.02 $m^2\ g^{-1}$. The mathematical formula used for the particle size distribution was a normalized Gamma distribution, according to Renforth et al (2015)[3]:

$$\Gamma(D) = \frac{D^{\alpha-1} e^{-D/\beta}}{\beta^{\alpha}\,\Gamma(\alpha)} \tag{4}$$

Coefficients α = 11.1 and β = 10.44 µm were obtained by non-linear least squares fitted to the grain size distribution data.

Prior to the experiments, the olivine sand was rinsed 10 times with 0.2 µm-filtered seawater, followed by one rinsing cycle with MilliQ water. Subsequently, the sand was dried at 80°C for 24 hrs. and stored until further use.

The lab-grade quartz (Merck Millipore, art. no. 107536) was reported as washed and calcined for analysis and had a median grainsize ($D_{50}$) of 324 ± 2.8 µm, with $D_{10}$ and $D_{90}$ quantiles of 167 ± 1 µm and 604 ± 5.5 µm, respectively, and contained less than 0.3 % of particles < 63 µm (mean ± SD are reported with n=4).

**Table S1**

The chemical composition of the olivine source material used in the experiments in this study. The mass fractions of the constituent metals were determined by ICP-OES analysis. Values calculated are in bold face.

| constituent | molar mass [g/mol] | mass fraction [g/kg olivine] | molar fraction [mol/kg olivine] | **stoichiometry [mol/mol $SiO_4$]** |
|---|---|---|---|---|
| Mg | 24.305 | 270.103 | 11.1131 | **1.8661** |
| Fe | 55.845 | 41.440 | 0.7421 | **0.1246** |
| Ni | 58.69 | 2.630 | 0.0448 | **0.0075** |
| Na | 22.99 | 0.359 | 0.0156 | **0.0026** |
| Ca | 40.08 | 0.074 | 0.0018 | **0.0003** |
| Cr | 52 | 0.048 | 0.0009 | **0.0002** |
| $SiO_4$ | 92.083 | **548.377** | **5.9552** | **1.0000** |

**Table S2**

The granulometric characteristics of the minerals used in this study. The median grainsize ($D_{50}$) and particle size distribution (psd) were determined with laser diffraction. The psd was used to calculate the geometric specific surface area ($A_{GEO}$). In addition, the specific surface area was determined using the B.E.T. method ($A_{BET}$). The $A_{GEO}$ and the $A_{BET}$ of the material differ an order of magnitude, which arises from the fact that to calculate the $A_{GEO}$, the particles are approximated as a perfect sphere or cube. This approximation disregards all sorts of surface irregularities, which add to the particle surface area[4].

| Mineral | $D_{10}$ [µm] (mean±SD) | $D_{50}$ [µm] (mean±SD) | $D_{90}$ [µm] (mean±SD) | $A_{GEO}$ [$m^2\ g^{-1}$] (mean) | $A_{BET}$ [$m^2\ g^{-1}$] (mean±SD) |
|---|---|---|---|---|---|
| Quartz (QUA) | 167 ± 1.2 | 324 ± 2.8 (n=6) | 604 ± 5.5 | 0.008 | not measured |
| Olivine (OLI) | 91 ± 0.3 | 143 ± 0.4 (n=6) | 224 ± 0.7 | 0.02 | 0.295 ± 0.1 (n=12) |

**Table S3**

The composition of the artificial seawater (ASW) stock mixtures used in experiment A3. All values are in mmol/kg seawater (SW), except for Total Alkalinity, which is given in μmol/kg SW.The aim was, in all cases, to make ASW mixtures with S=30, pH=7.95 and TA=2450 μmol/kg. Total Alkalinity (TA) was determined by potentiometric titration, while salinity (S) was measured conductometrically.

| component | ASW | ASW-Ca | ASW-CaMg |
|---|---|---|---|
| NaCl | 416.15 | 423.62 | 474.26 |
| KCl | 8.87 | 8.79 | 11.04 |
| $CaCl_2 \cdot 2H_2O$ | 9.13 | | |
| $MgCl_2 \cdot 6H_2O$ | 22.6 | 22.36 | |
| $MgSO_4 \cdot 7H_2O$ | 25.1 | 24.78 | |
| $Na_2SO_4$ | | | 7.23 |
| $NaHCO_3$ | 2.401 | 2.409 | 2.465 |
| total salts | 484.25 | 481.96 | 494.995 |
| Salinity (S) | 30.21 | 29.81 | 30.09 |
| Total Alkalinity (TA) | 2384.13 | 2440.01 | 2446.92 |
| pH | 7.94 | 7.95 | 8.01 |
| ionic strength | 0.72 | 0.705 | 0.623 |

## SI 3: Overview of experimental conditions

### Table S4

Overview of the experimental details of the three Agitation experiments A1, A2 and A3. The sampling days represents the days on which the overlying water was sampled according to the described methodology. Treatments consist of either minerals added or seawater control: OLI = olivine treatment, QUA = quartz treatment, SW = seawater (control) treatment. The reactive fluid is the medium in which dissolution took place: FSW = Filtered natural Seawater, ASW = Artificial Seawater, ASW-Ca = Artificial Seawater without Calcium, ASW-CaMg = Artificial Seawater without Calcium and Magnesium. The reactive fluids in experiments A2 and A3 were air-bubbled prior to the experiment in order to equilibrate them with ambient $CO_2$. This procedure was not done in experiment A1. Also in experiments A2 and A3, the temperature was controlled within a far narrower range, compared to A1.

| experiment | sampling [days] | temp. [°C] | *p*CO2 [ppm] | treatment | replicates [n] | mass added [g] (mean±SD) | reactive fluid |
|---|---|---|---|---|---|---|---|
| A1 | 0, 5, 12, 15, 54, 88 | 13.5-20 | 445-525 | OLI | 4 | 15.33 | FSW |
| | | | | QUA | 4 | 6.01 | FSW |
| | | | | SW | 4 | - | FSW |
| A2 | 0, 6, 13, 20 | 17.7 ± 0.5 | 444 ± 22 | OLI | 3 | 15.33 | FSW |
| | | | | QUA | 3 | 6.09 | FSW |
| | | | | SW | 3 | - | FSW |
| A3 | 0, 2, 4, 7, 10, 14, 20, 30, 137 | 17.5 ± 0.2 | 384 ± 21 | OLI | 3 | 4.59 | FSW |
| | | | | SW | 3 | - | FSW |
| | | | | OLI | 3 | 4.59 | ASW |
| | | | | SW | 3 | - | ASW |
| | | | | OLI | 3 | 4.6 | ASW-Ca |
| | | | | SW | 3 | - | ASW-Ca |
| | | | | OLI | 3 | 4.6 | ASW-CaMg |
| | | | | SW | 3 | - | ASW-CaMg |

### Experimental details

The solid phase (olivine or quartz particles) was subjected to constant agitation in different reactive fluids (see Table S3 below). The reaction vessels, 500 mL boro-silicate glass bottles with 0.5 mm silicone membrane screw caps, were placed on a CH-4103 rotating shaking platform (INFORS AG, Switzerland) set at 155 rpm. Although the agitation by itself is meant to resemble natural agitation by wave action, the chosen value for revolutions per minute (rpm) was chosen "by eye": there needed to be a constant agitating effect by the rotation, so that olivine particles would be subject to constant water motion, but not be so strong that the water would keep the particles constantly resuspended. This was done by trial and error, until values between 150 and 160 rpm were found adequate.

In the first two experiments A1 and A2, a plateau in ΔTA was reached relatively fast, within a matter of days. In experiment A3 a lower amount of olivine was used, to postpone the leveling off and therefore to better study the process.

As an additional control for the seawater movement, a layer of olivine sand was placed in a non-moving cylindrical container with FSW (n=1), of which the overlying water was stirred. From this non-agitated treatment only samples for solid phase analysis were collected.

**Sample treatment**

On each sampling occasion, a 40 ml aliquot of the overlying supernatant was sampled and distributed into separate containers for the following analyses:

1. 14 ml for total alkalinity (TA) analysis in a 15 ml centrifuge tube (TPP, Switzerland)
2. 10 ml for dissolved inorganic carbon (DIC) analysis in a 10 ml glass headspace vial. Samples for DIC analysis were poisoned with 1 µl 0.24 M $HgCl_2$ per ml sample to arrest all biological reactions.
3. 10 ml for dissolved metals analysis in a 15 ml centrifuge tube (TPP, Switzerland)
4. 5 ml for dissolved silicate in a 6 ml nutrient vial

All vials were stored at 4°C until further analysis.

**Water phase chemical analyses**

The *p*H was measured on each sampling occasion, by insertion of an Orion 8102BN ROSS electrode (Thermo Scientific) connected to a Keithley 617 programmable electrometer. The *p*H electrode was calibrated using commercial NBS 4 and NBS 7 *p*H buffers (Merck) and self-pepared TRIS buffer. The *p*H values are reported on the total scale. Salinity was measured for each individual sample, prior to the alkalinity titrations, using a CDM230 conductivity meter (Radiometer Analytical). Potentiometric titrations for Total Alkalinity (TA) were performed using an automated Titrando titration setup (Metrohm AG, Germany). DIC analyses were done by acidifying each sample, causing all dissolved $CO_2$ species to be converted to gaseous $CO_2$. The outgassed $CO_2$ was subsequently led over an infrared gas analyser Li-7000 $CO_2/H_2O$ Analyser (Apollo SciTech, Lincoln, USA).

Dissolved silicon (Si) and dissolved magnesium ($Mg^{2+}$) are the major ions released during forsteritic olivine dissolution. However, seawater has an elevated background concentration of $Mg^{2+}$ (~50 mmol kg-1), against which the expected release (in this experiment, on the order of 0.001 mmol $kg^{-1}$) would not be detected over the analytical error of the instrument. One of the conspicuous metals in forsteritic olivine is nickel, and its natural background concentration in seawater is low. Therefore, dissolved nickel was used as a secondary proxy to measure olivine dissolution.

Dissolved silicate (DSi), was measured spectrophotometrically using a QuAAttro automated microflow analyzer (SEAL Analytical). Dissolved metals (DMg, DCa) were analysed on an iCAP 6000 series ICP-OES (Thermo Scientific). Samples for dissolved Nickel (DNi) analysis were acidified with 50 µL per mL of sub-boiled distilled $HNO_3$ (65%) and preserved at 4°C. The analysis was done by High Resolution - Inductively Coupled Plasma – Mass Spectroscopy (HR-ICP-MS, ThermoScientific Element 2) after 20x dilution with Milli-Q. Indium (2.5 ppb) containing 2% $HNO_3$ was injected simultaneously with the samples as internal standard. To account for matrix effects, the linear slope of the external calibration was corrected with the linear slope of the internal

calibration (i.e. standard addition) of 1 sample [5].

**Solid phase analysis**

Upon completion of the A3 experiment, the solid phase was analysed for potential carbonate precipitation. To this end, the solid phase in A3 and the "no shake" treatments was recovered, rinsed with distilled water, dried at 80°C for 24 h, and stored dry until further analysis. The sample was analysed for carbon (C; as a proxy for carbonate) on an CHNS/O Elemental Analyser (Eurovector, Milan, Italy), treated with and without HCl treatment before analysis, according to Nieuwenhuize et al. [6]. The difference between the two measurements is the inorganic carbon content, which we interpret as carbonates ($CaCO_3$, $MgCO_3$ or mixed carbonate minerals). The results are given as mass percentage inorganic carbon (mass% $C_{inorg}$). For subsequent statistical analysis, the mass% data were arcsine-square root transformed [7].

Olivine grains recovered from all treatments in experiment A3 were also inspected for dissolution features. The grain surface of olivine particles was investigated using a scanning electron microscope (Hitachi TM3030) coupled to energy-dispersive X-ray spectroscopy (Hitachi SwiftED3000). Per treatment, multiple grains were analysed, and between 8 and 20 sub-areas per grain were scanned. Fresh, untreated olivine minerals served as a control substrate.

To investigate the alteration of primary minerals or formation of secondary minerals, X-ray diffraction (XRD) analysis was performed on the recovered solid phase of the A3 experiment. The XRD analyses were done using a STADI MP diffractometer (STOE, Darmstadt, Germany), in reflection (Bragg-Brentano geometry) with primary monochromator (Germanium) and linear Position Sensitivity Detector (PSD). The used Cu/K wavelength was $\alpha 1$ = 1,5406 Å, the step length was 0.005° $2\theta$ (2 Theta) and the count time was 150 seconds.

## SI 4: Calculation of dissolution rate constants

The accumulation over time of the reaction products in the reactor vessels is reported as excess concentration values, $\Delta C(t) = C_{treatment}(t) - C_{control}(t)$, where the control is the reactive fluid (seawater medium) without the addition of any solid minerals. Three different mathematical relations were implemented to describe the accumulation of reaction products as a function of the incubation time (Table S5, first column). These three empirical models were fitted to the data by non-linear least squares regression analysis (nls function in R). Best model fits (Fig. S5) were selected by comparison of Akaike's Information Criterion [7]. Figure S6 shows two representative examples of model fits.

**Table S5**

Three empirical models were used to describe the accumulation of olivine dissolution reaction products (Eqs. 1, 2 and 3). The time derivative at time t=0 is given in the right-hand column, which is used to calculate the initial accumulation rate $R_0$ (Eqs. 4, 5 and 6).

| Accumulation model | Initial accumulation rate |
|---|---|
| (1) Linear: $\Delta C(t) = a \cdot t$ | (4) $R = a$ |
| (2) Saturation: $\Delta C(t) = \Delta C^{max}\left(1-\exp(-b \cdot t)\right)$ | (5) $R = b \cdot \Delta C^{max}$ |
| (3) Combined: $\Delta C(t) = a \cdot t + C^{max}\left(1-\exp(-b \cdot t)\right)$ | (6) $R = a + b \cdot \Delta C^{max}$ |

**Figure S6** Examples of model fits in which (left panel) there is no justification for fitting the more complex combined model against the data, thus accepting the saturation model, and (right panel) in which there is visually (and numerically) a better fit with the more complex, combined model.

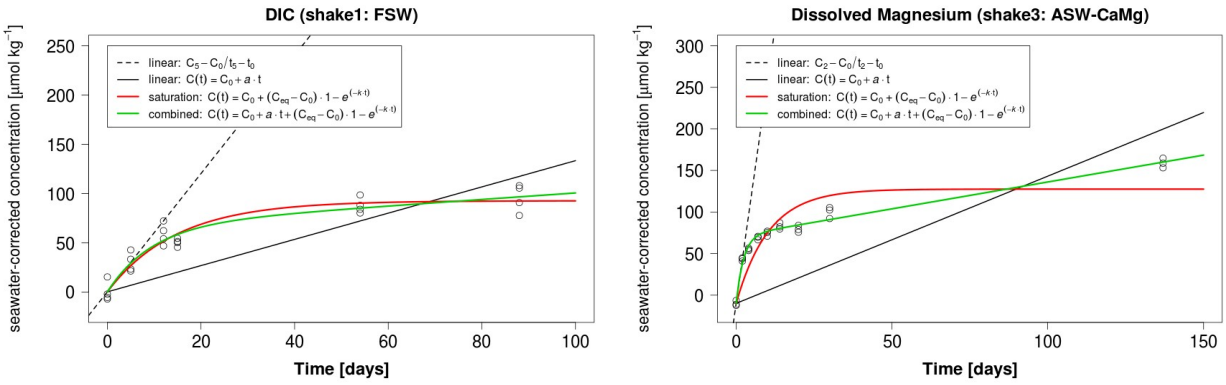


The accumulation rate of a given substance *i* in the supernatant solution is defined as $R_i(t) = d\Delta C_i(t) / dt$ expressed in µmol substance $kg^{-1}$ seawater $d^{-1}$ (Table S5, second column). The relation with the area-specific dissolution rate constant $k_i$, of olivine (expressed in µmol per $m^2$ surface area per day: [µmol $m^{-2}$ $d^{-1}$]) is given by:

$$(5) \qquad R_i = k_i \cdot v \cdot A_{sp} \cdot (1/\rho_{sw})(m/V_{sw})$$

where $A_{sp}$ is the specific surface area [$m^2$ $g^{-1}$], $\rho_{sw}$ is the density of the supernatant solution, *m* the

dry mass [g] of the mineral added to the slurry, and $V_{sw}$ is the solution volume added to the reaction vessel [$m^3$]. The quantity $v$ represents the stoichiometric coefficient of the specific reaction product in the reaction equation of olivine dissolution (Si=1; $Mg^{2+}$=1.87; TA=4; Ni=0.0075; Table S1). In the case of congruent (i.e. stoichiometric) dissolution, and no secondary reactions, the olivine dissolution rate constant should be identical for all response variables. When these conditions are not met, the $k_i$ will depend upon the substance monitored (as is the case here).

The dissolution experiments showed saturation behavior, implying that $k_i(t)$ decreases with time. To exclude these saturation effects, we calculated the reported dissolution rate constants $k_i$ from the initial accumulation rate $R_i(t=0)$, via the relation:

$$k_i = \frac{R_i(t=0)}{v \cdot A_{sp} \cdot (1/\rho_{sw})(m/V_{sw})} \quad (6)$$

The dissolution experiments in this study were performed at a temperature of 17°C, while dissolution rate constants are typically reported at 25°C (Hangx and Spiers 2009, and references therein). To enable a comparison with previously reported literature values, the $k_i$ rate constants were rescaled to 25°C according to the Arrhenius equation:

$$k_1/k_2 = e^{\Delta E_a/R_G T_1} / e^{\Delta E_a/R_G T_2} \quad (7)$$

Here, $\Delta E_a$ = 79.5 [kJ $mol^{-1}$] is the activation energy [8], $R_G$ = [8.314 J $K^{-1}$ $mol^{-1}$] is the gas constant and $T_i$ is absolute temperature in Kelvin. This relation implies that the dissolution rate constant at the reference temperature of 25°C is a factor 2.42 higher than its value at 17°C.

All mathematical analyses and plotting were done using R, the open source framework for statistical computing [9]

**SI 5: Model simulations**

The accumulation of weathering products in the slurry experiments was simulated using the geochemical software package PHREEQC v2 [10], using the LNLL.dat database, to derive the saturation states of solid phases in the solution. PHREEQC (using the minteq.dat database) was also used to model the kinetics of forsterite dissolution, set up with initial conditions specific to each experimental condition ( (known/estimated concentrations of Na, K, Mg, Ca, Cl, $SO_4$, $HCO_3$, and Si, pH, mineral surface area, temperature). The rate of forsteritic olivine dissolution ($r$, mol $m^{-2}$ $s^{-1}$) was simulated using the rate formulae from the standard work of Palandri and Kharaka (2004)[11] :

$$(5)\quad r = A_s \cdot m_V \left( k_a \alpha_{H^+}^{0.47} (1-\Omega) e^{x} \right) + \left( k_n (1-\Omega) e^{y} \right)$$

$$(6)\quad x = \frac{E_a}{R}\left(\frac{1}{T} - \frac{1}{298.15}\right), y = \frac{E_n}{R}\left(\frac{1}{T} - \frac{1}{298.15}\right)$$

Where $k_a$ ($10^{-6.86}$) and $k_n$ ($10^{-10.65}$) are the acid and neutral rate constants for fosterite dissolution, respectively [mol $m^{-2}$ $s^{-1}$], $\alpha_{H+}$ is the hydrogen ion activity, and $\Omega$ is the saturation state of forsterite in solution, $E_a$ (-67.2) and $E_n$ (-79.0) are the acid and neutral activation energies [kJ $mol^{-1}$] of fosterite, $R$ is Avogadro's gas constant, and T is solution temperature [K] [11]. $A_s$ is surface area of the material ($m^2$ $g^{-1}$) and $m_V$ is the mass of mineral per volume of solution. The PHREEQC kinetic model results for $\Delta$Si showed that using the geometrically-calculated specific surface area (0.02 $m^2$ $g^{-1}$), rather than B.E.T.-determined surface area (0.3 $m^2$ $g^{-1}$), yielded results more similar to the actual measured Si concentrations (see below).

**Figure S7.** Comparison of measured values for ΔSi against PHREEQC model results using either the geometrically-derived surface area of the olivine (A_geo) or the BET-derived surface area (A_BET). **(A)** = Experiment A1: FSW; **(B)** = Experiment A2: FSW; **(C)** = Experiment A3: ASW; **(D)** = ASW-Ca; **(E)** = Experiment A3: ASW-CaMg. The red circles denote measured ΔSi values. Black lines depict PHREEQC modelled ΔSi values using A_BET, while grey lines depict PHREEQC modelled ΔSi values using A_geo.

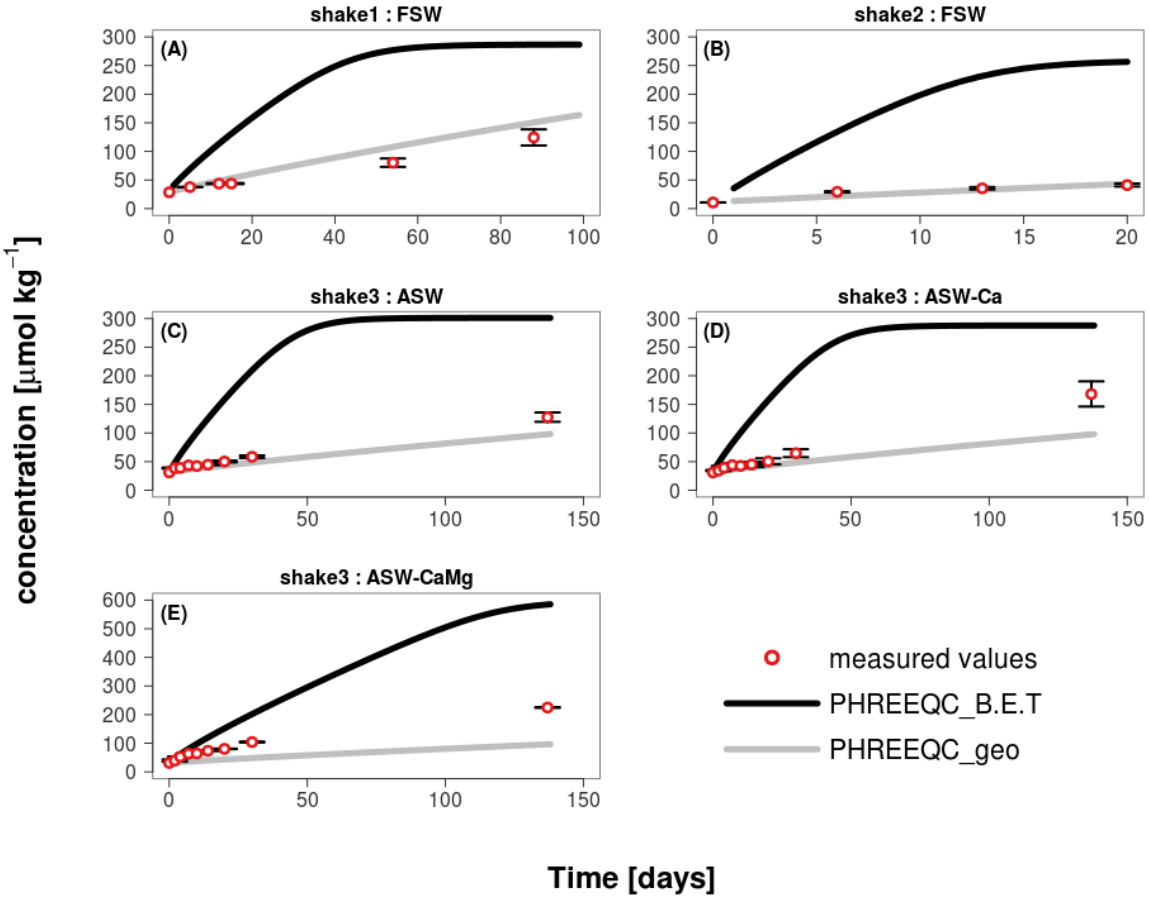

## SI 6: Accumulation of reaction products in experiment A3

**Figure S8.** Accumulation of reaction products normalized for their stoichiometry as reported in Table S2 (ΔSi/1, ΔTA/4, ΔNi/0.0075, ΔMg/1.87). Each panel shows the results for a different seawater medium (FSW, ASW, ASW-Ca and ASW-CaMg) in experiment A3. Note that only in the ASW-CaMg treatment (bottom-right panel), ΔMg could be measured, as the background concentration [$Mg^{2+}$] was sufficiently low to reliably detect the ΔMg signal. of the solvent media FSW, ASW, ASW-Ca and ASW-CaMg, in experiment A3.

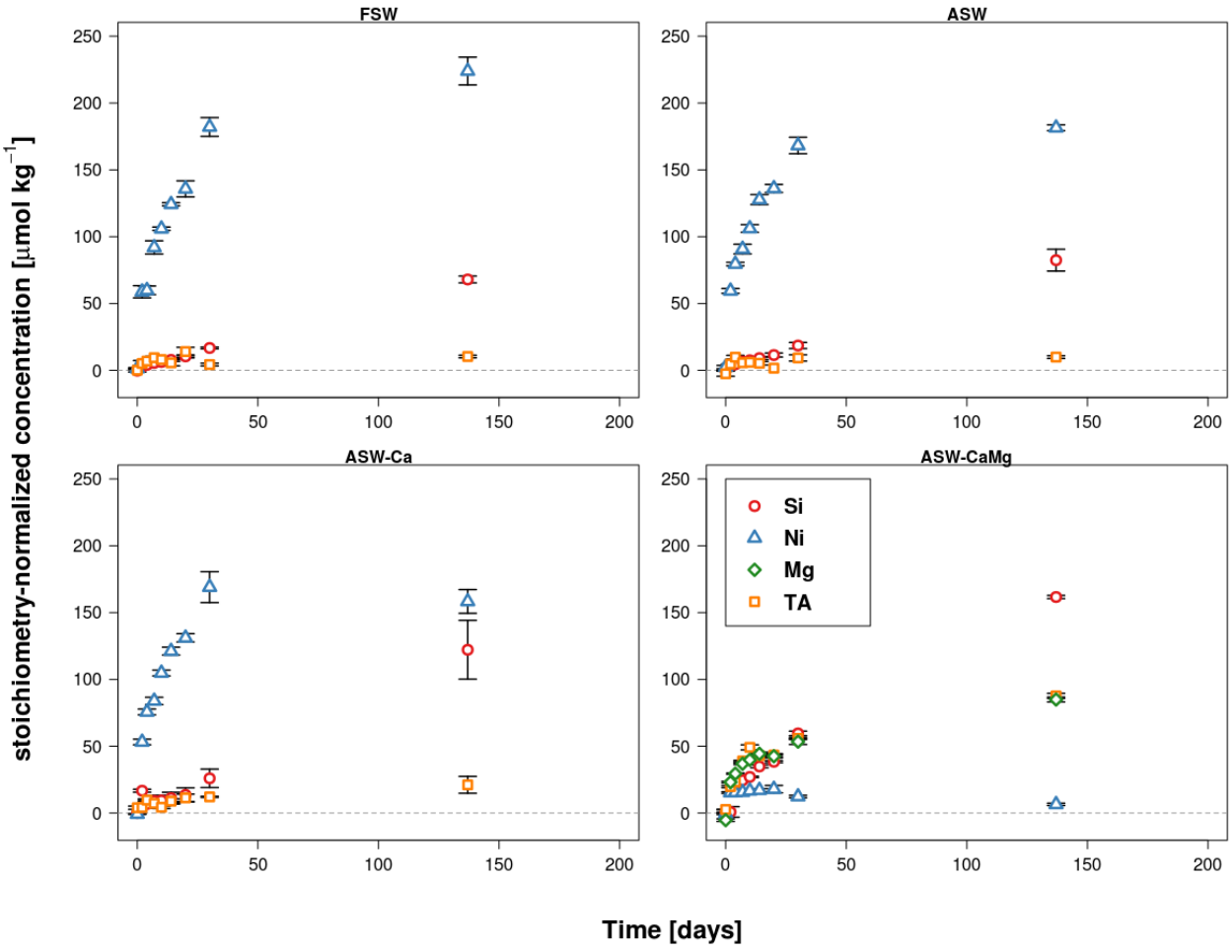

## SI 7: Solid phase analysis

### Olivine particle surface Mg:Si atomic ratio

To determine (in)congruent dissolution, the atomic ratio of Mg:Si at the surface of olivine particles was investigated. Figure S9 shows that the Mg:Si range of the unreacted source material (substrate) ranges between 1.8 and 2.5, with both mean and median around 2.1. Because of heteroscedasticity of the data (non-homogeneity of variances), even after log-transformation, a non-parametric Kruskal-Wallis rank sum test was performed. There were significant differences in Mg:Si ratio between the substrate and most of the reacted materials (Kruskal-Wallis, $\chi^2 = 85.6828$, df=4, p<<0.0001). A Tukey's HSD *post-hoc* test of log-normal transformed Mg:Si ratios (lnMg:Si), revealed no significant differences between the unreacted substrate olivine and the "no shake" olivine (see Methods; p = 0.9999; Fig. 5) and between the unreacted olivine and that from the ASW treatment (p = 0.8169). However, the Mg:Si of the olivine of the FSW and especially that of the ASW-CaMg treatment were both significantly lower (Tukey's HSD, p = 0.0072 and p << 0.0001, respectively). Moreover, the range of Mg:Si values of the latter treatment was considerably larger, extending to lower values and even falling below 1 (Fig. S8 below).

**Figure S9.** Box-whisker plot of the Mg/Si ratio of sampled olivine grains. The thick black line in the boxes denotes the median value, while the green diamonds denote the means. The open circles are statistical outliers. The capital letters above the boxes show the clustering of group means according to a Tukey HSD post-hoc test. Means denoted by the same letters are not significantly different, while those denoted by two or more letters overlap. The width of the boxes is proportional to the sample size. The treatments considered are: substrate = unreacted olivine; non-agitated = treatment control, in which the olivine was not agitated, but only in contact with moving filtered seawater; FSW = Filtered Seawater treatment A3; ASW = Artificial Seawater treatment A3; ASW-CaMg = Artificial Seawater without Calcium and Magnesium treatment A3.

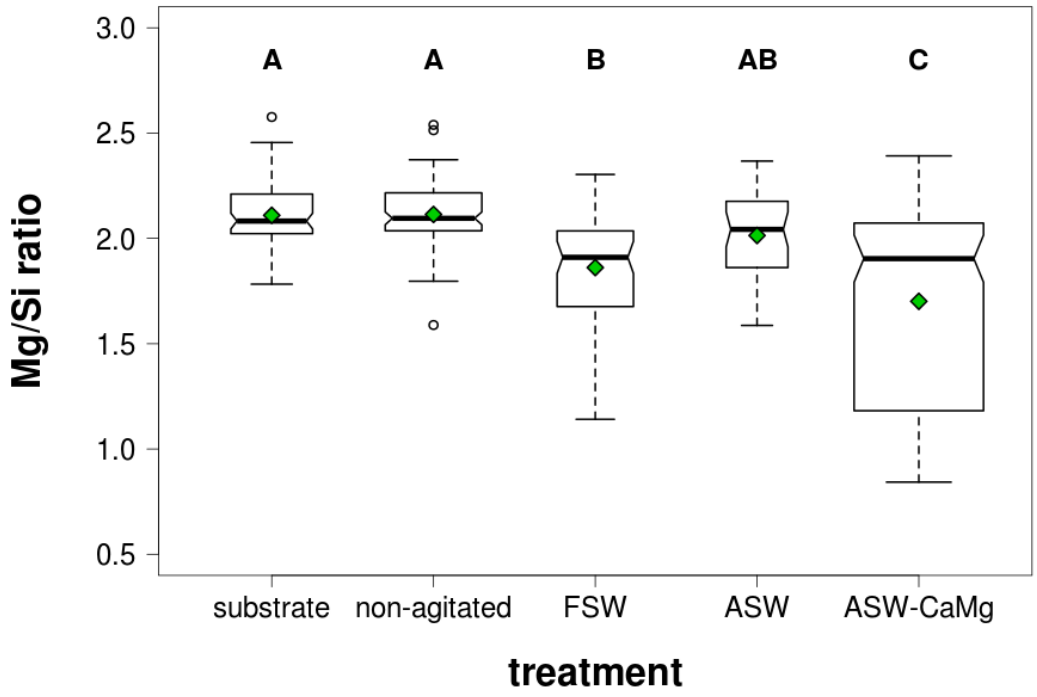

**Figure S10**. SEM-EDX micrograph of an olivine particle, subjected to continuous movement and dissolution in the calcium and magnesium-free artificial seawater medium (ASW-CaMg) during the 137-day experimental period. Rounded surface features can be seen. A sodium chloride crystal (from seawater), characterized by high Na and Cl values, could be discerned (Area 1). In addition, the olivine particle is characterized by large regions where the Mg:Si atomic ratio approaches 1 and sometimes even falls below 1 (Areas 2). These areas represent strong chemical weathering, with preferential leaching of metal ions caused by the negligible presence of divalent cations in the ASW-CaMg medium. Note the appearance of the particle surface, where a layered structure or flakes seems to have formed. In the center of the bottom Area 2, these layered structures seem to have been removed.

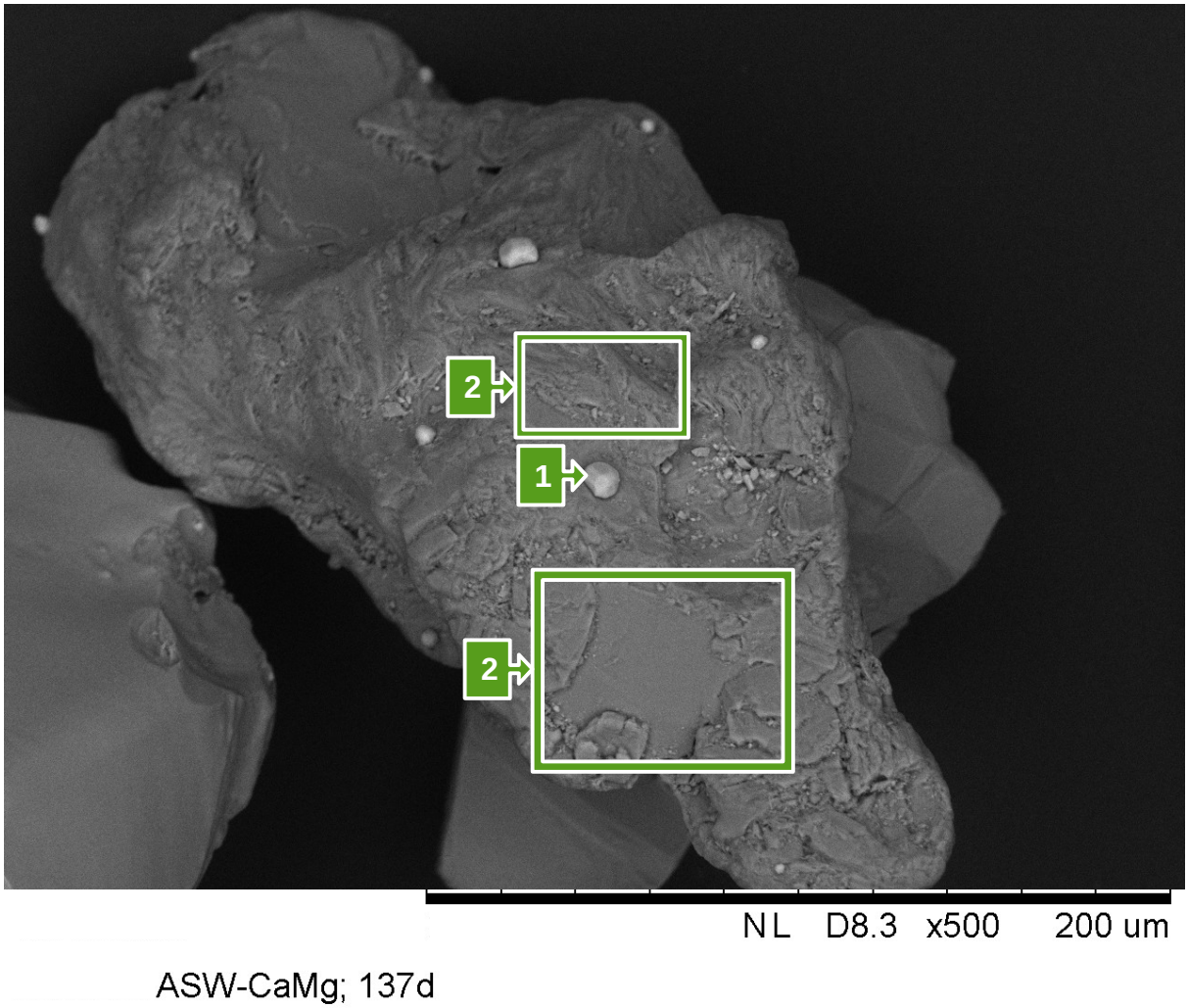

The mass percentage of inorganic carbon (mass% $C_{inorg}$) in the solid mineral phase recovered from experiment A3 was both very low and not significantly different between the four treatments (one-way ANOVA, p=0.112). At these specifically low $C_{inorg}$ values, the analytical uncertainty is ca. 5%. The arcsin(sqrt x+1)-transformed data showed no sign of heteroscedasticity according to both a Fligner-Killeen test (p = 0.119) and a Bartlett test (p = 0.14).

The mean±SEM mass% $C_{inorg}$ values were 0.0038 ± 0.0013 for FSW, 0.027 ± 0.0006 for ASW, 0.029 ± 0.0007 for ASW-Ca and 0.0009 ± 0.0005 for ASW-CaMg (Fig. S10 below).

**Figure S11.** Mean±standard deviation (SD) of the mass percentage of inorganic carbon (mass% $C_{inorg}$) for all four treatments, measured in the solid mineral phase recovered at the end of experiment A3. The treatments considered here are: FSW = Filtered Seawater treatment; ASW = Artificial Seawater treatment; ASW-Ca = Artificial Seawater without Calcium treatment; ASW-CaMg = Artificial Seawater without Calcium and Magnesium treatment. Although the mass% $C_{inorg}$ appears to be lower in the ASW-CaMg treatment, a one-way ANOVA demonstrated this difference to be non-significant ($F$ = 2.267; df = 3, 20; p = 0.112).

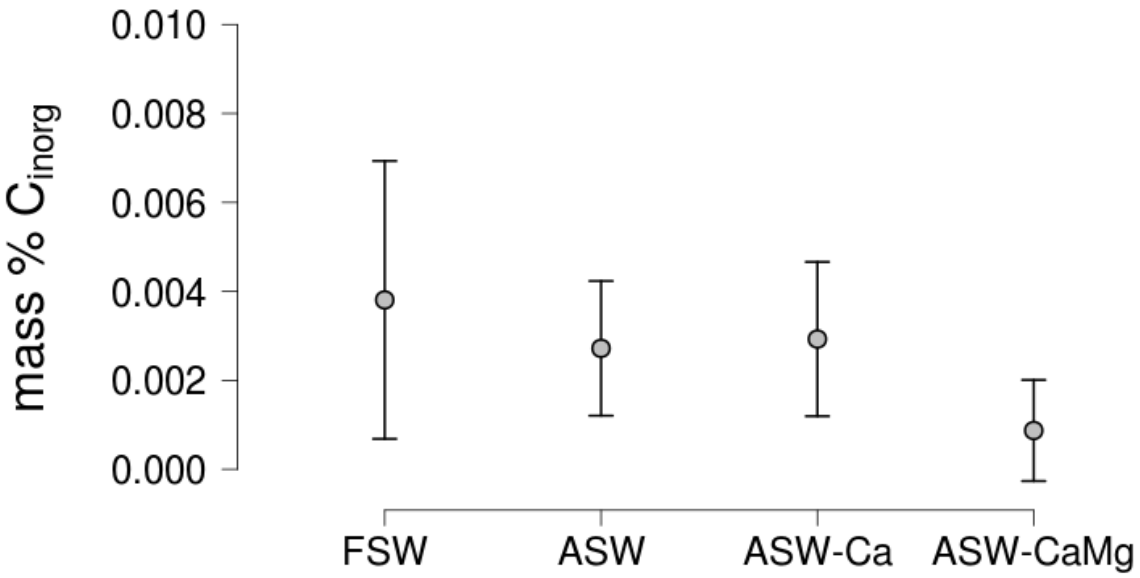

## SI 8: Calculation of total mass olivine weathered and $CO_2$ captured

Using the Olsen[12] shrinking core model for olivine carbonation[13], the total mass of olivine weathered and consequential $CO_2$ captured can be modeled. The obtained $k$ value (here: $k_{\Delta TA}$= 16.51 μmol $m^{-2}$ $d^{-1}$) is converted into a weathering rate, yielding 0.26 μm $year^{-1}$.

The experimental olivine is divided into 11 size classes, according to the particle size distribution in SI 2, from which the total mass per size class can thus be calculated. For each time step (year), the weathering rate per size class is calculated, feeding the Olsen[54] shrinking core model. According to the yearly weathering, particles will decrease in size and may fall in smaller size class for the next year. As such, the mean particle diameter can be calculated leading to the total mass of particles in a given size class for the next time step. With the shrinking core model, the total mass weathered per size class is calculated, and summed over all size classes to yield the yearly total weathered mass of olivine. This can then be converted into total mass $CO_2$ captured per year, using Eqn. (6) : $R_{CO_2} = 4\, R_{OLI}\, \gamma_{CO_2} (1-x)$ .

**SI 9: References**


(1) Köhler, P.; Hartmann, J.; Wolf-Gladrow, D. A. Geoengineering potential of artificially enhanced silicate weathering of olivine. *Proc. Natl. Acad. Sci. U. S. A.* **2010**, *107* (47), 20228–20233.

(2) Renforth, P.; Jenkins, B. G.; Kruger, T. Engineering challenges of ocean liming. *Energy* **2013**, *60*, 442–452.

(3) Renforth, P.; Pogge von Strandmann, P. A. E.; Henderson, G. M. The dissolution of olivine added to soil: Implications for enhanced weathering. *Appl. Geochemistry* **2015**, *61*, 109–118.

(4) *Kinetics of Water-Rock Interaction*; Brantley, S. L., Kubicki, J. D., White, A., Eds.; Springer-Verlag: New York, 2008.

(5) Milne, A.; Landing, W.; Bizimis, M.; Morton, P. Determination of Mn, Fe, Co, Ni, Cu, Zn, Cd and Pb in seawater using high resolution magnetic sector inductively coupled mass spectrometry (HR-ICP-MS). *Anal. Chim. Acta* **2010**, *665*, 200–207.

(6) Nieuwenhuize, J.; Maas, Y. E. .; Middelburg, J. J. Rapid analysis of organic carbon and nitrogen in particulate materials. *Mar. Chem.* **1994**, *45* (3), 217–224.

(7) Quinn, G. P.; Keough, M. J. *Experimental design and data analysis for biologists*, 1st ed.; Cambridge University Press: Cambridge, 2002.

(8) Wogelius, R. A.; Walther, J. V. Olivine dissolution kinetics at near-surface conditions. *Chem. Geol.* **1992**, *97* (1–2), 101–112.

(9) R Development Core Team. R: A language and environment for statistical computing. R Foundation for Statistical Computing: Vienna, Austria 2008.

(10) Parkhurst, D. L.; Appelo, C. A. J. User's guide to PHREEQC (Version 2): A computer program for speciation, batch-reaction, one-dimensional transport, and inverse geochemical calculations. United States Geological Survey 1999.

(11) Palandri, J. L.; Kharaka, Y. K. *A compilation of rate parameters of water-mineral interaction kinetics for application to geochemical modeling*; Menlo Park, California, 2004; Vol. 2004–1068.

(12) Olsen, A. A. Forsterite dissolution kinetics: Applications and implications for chemical …, Virginia State University, 2007.

(13) ten Berge, H. F. M.; van der Meer, H. G.; Steenhuizen, J. W.; Goedhart, P. W.; Knops, P.; Verhagen, J. Olivine Weathering in Soil, and Its Effects on Growth and Nutrient Uptake in Ryegrass (Lolium perenne L.): A Pot Experiment. *PLoS One* **2012**, *7* (8), e42098.